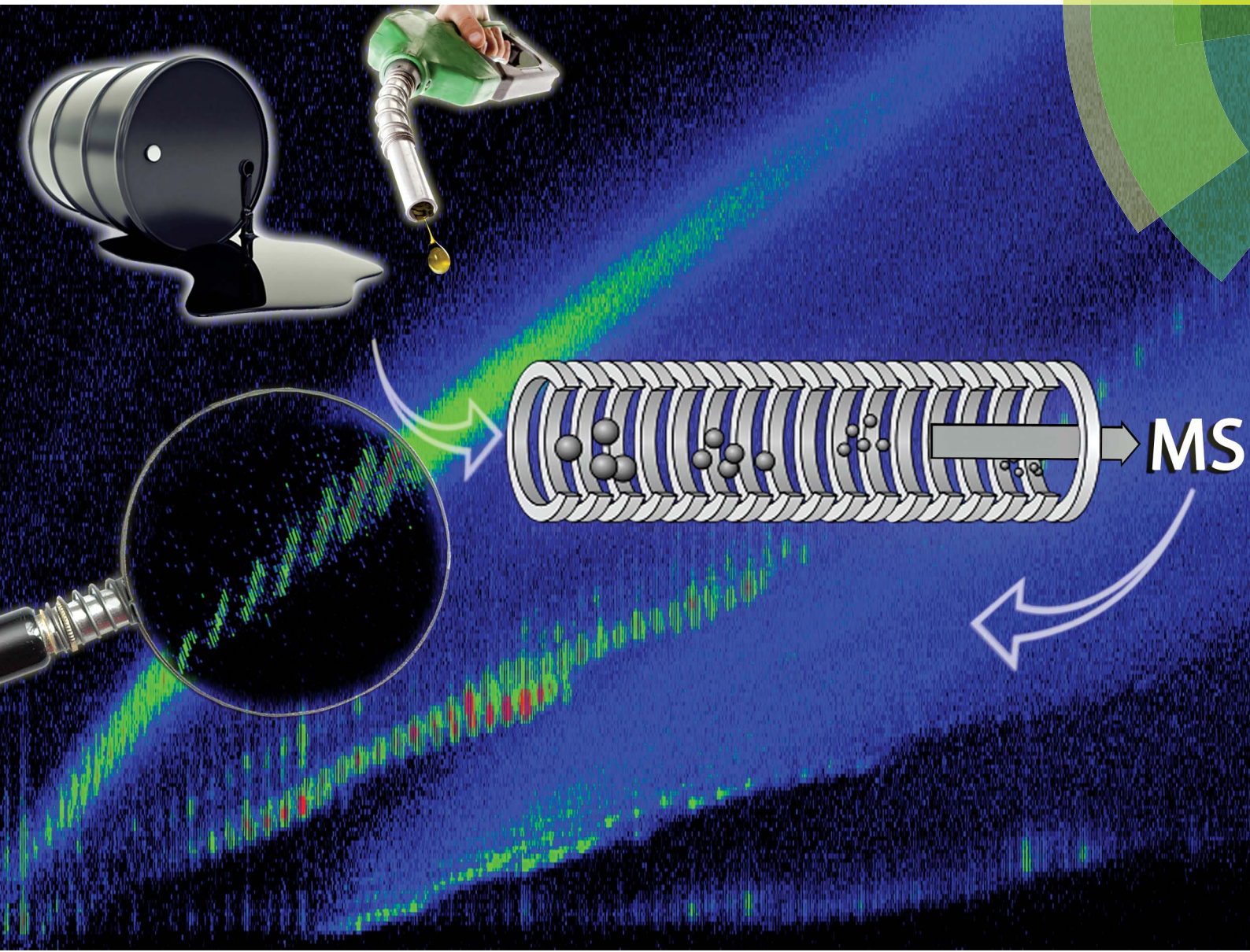


# Analytical Methods

[www.rsc.org/methods](http://www.rsc.org/methods)



ISSN 1759-9660



PAPER

Jandyson Machado Santos *et al.*

Petroleomics by ion mobility mass spectrometry: resolution and characterization of contaminants and additives in crude oils and petrofuels



Cite this: *Anal. Methods*, 2015, 7, 4450

## Petroleomics by ion mobility mass spectrometry: resolution and characterization of contaminants and additives in crude oils and petrofuels†

Jandyson Machado Santos,<sup>\*a</sup> Renan de S. Galaverna,<sup>a</sup> Marcos A. Pudenzi,<sup>a</sup> Eduardo M. Schmidt,<sup>a</sup> Nathaniel L. Sanders,<sup>b</sup> Ruwan T. Kurulugama,<sup>b</sup> Alex Mordehai,<sup>b</sup> George C. Stafford,<sup>b</sup> Alberto Wisniewski, Jr<sup>c</sup> and Marcos N. Eberlin<sup>a</sup>

Ion mobility-mass spectrometry (IM-MS), performed with exceptional resolution and sensitivity in a new uniform-field drift tube ion mobility quadrupole time-of-flight (IM-QTOF) instrument, is shown to provide a useful tool for resolving and characterizing crude oils and their contaminants, as well as petrofuels and their additives. Whereas direct analysis of a crude oil sample contaminated with demulsifiers by the classical ESI(±)-FTICR-MS petroleomic approach was unsatisfactory since it responds only with abundance and *m/z*, and ionization is impaired due to suppression of polar compounds of crude oil by additives likely used in petroleum industry, IM-MS enables mobility separation of ions, particularly of double bond equivalent (DBE) series for a giving  $C_nX$  class providing separated spectra which are typical obtained either for the crude oil or the contaminants, even suffering of ion suppression or low ionization efficiency. The combination of improved IM resolution and high mass resolving power (40,000@400) of the QTOF instrument provides useful information on class (N, NO, NS, etc.), carbon number ( $C_n$ ), and unsaturation (DBE) levels for crude oils, allowing one to infer geochemical properties from DBE trends that can be compared with IM-MS data. As demonstrated by results of gasoline samples with additives, the IM-MS system also allows efficient separation and characterization of additives and contaminants in petrofuels.

Received 29th January 2015

Accepted 23rd April 2015

DOI: 10.1039/c5ay00265f

[www.rsc.org/methods](http://www.rsc.org/methods)

## 1. Introduction

A petrochemical sample can be considered well-defined only when the composition of its myriad of constituents from many different classes, polarities and unsaturation levels is comprehensively known.<sup>1</sup> Crude oils are known to be composed predominantly of hydrocarbons<sup>2</sup> but a minor (*c.a.* 5–15%) and important class is that of polar compounds containing heteroatoms such as N, S, and O. Whereas these polar compounds are normally associated with problems in the petroleum industry such as the corrosion, catalyst poisoning, coke formation, and undesired emulsions,<sup>2–4</sup> they also serve as important classes of petromarkers in crude oil studies. Ultra-high resolution and accuracy Fourier transform mass spectrometry and electrospray ionization analysis, both in the positive and negative ion modes [ESI(±)-FTICR-MS], are normally employed,<sup>5</sup> and the information

collected on these polar compounds are used to predicted important geochemical properties of the petroleum such as origin,<sup>6</sup> biodegradability,<sup>7</sup> thermal evolution,<sup>8</sup> and total acid number.<sup>9</sup>

For crude oils, the formation of water-in-crude oil emulsions is a common problem in the petroleum industry,<sup>10,11</sup> and demulsifiers<sup>12,13</sup> such as nonionic surfactants, often composed of polymers of ethylene oxide (EO) and propylene oxide (PO)<sup>13–16</sup> are sometimes added to crude oil during storage and transportation and compose samples submitted to chemical characterization. Gas chromatography combined with mass spectrometry (GC-MS) has been the primary technique used to characterize crude oil but is mostly limited to hydrocarbons.<sup>17</sup> Polar components<sup>18</sup> are less suitable for direct GC,<sup>1</sup> hence direct fingerprinting analysis *via* ESI-FTCR-MS,<sup>19</sup> TOF-MS<sup>20</sup> or Orbitrap MS<sup>21</sup> have been used in a field which is known as petroleomic MS.<sup>5</sup> Such approaches based on exact mass measurements and formula attribution can characterize many polar components of crude oils according to carbon number, heteroatom class, and unsaturation levels as measured by the double bond equivalent (DBE) index,<sup>22</sup> but more refined structural analysis are not provided.

Ion mobility techniques, combined with MS (IM-MS), incorporate shape and size as additional dimensions of structural investigation of gaseous ions<sup>23,24</sup> and have therefore been

<sup>a</sup>ThomSon Mass Spectrometry Laboratory, State University of Campinas – UNICAMP, Institute of Chemistry, Campinas, São Paulo, 13083-970, Brazil. E-mail: jandyson.machado@gmail.com; Tel: +55 19 3521-3073

<sup>b</sup>Agilent Technologies, Santa Clara, CA 95051, USA

<sup>c</sup>Federal University of Sergipe, Department of Chemistry, São Cristóvão, Sergipe, 49100-000, Brazil

† Electronic supplementary information (ESI) available. See DOI: 10.1039/c5ay00265f

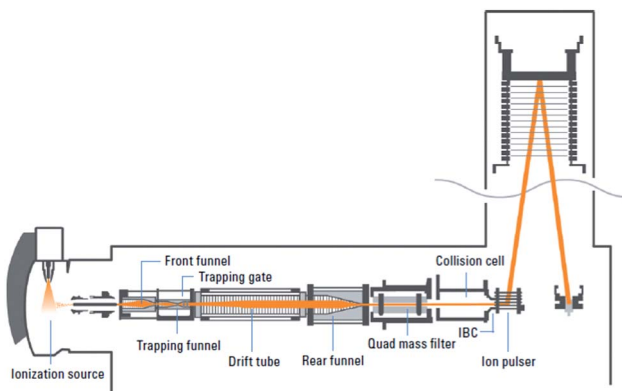


Fig. 1 Schematics of the Agilent 6560 ion mobility quadrupole time-of-flight (IM-QTOF) mass spectrometer.

applied as a complementary technique for comprehensive crude oil characterization. In IM, ions are separated as they drift through a “static” gas under the influence of an external electric field.<sup>17</sup>

In the past, IM-MS experiments were restricted to home-made instruments,<sup>25–27</sup> until the first commercial IM-MS spectrometer became available in 1971.<sup>28</sup> In 2004, an innovative IM system using a much more compact and high transmission travelling wave IM cell (TWIM) was introduced.<sup>29</sup> A few years latter, a 2<sup>nd</sup> generation TWIM system employing a longer (*c.a.* 25.2 cm) cell with improved IM resolution IM (Rp 40) was introduced.<sup>30</sup> The application of the TWIM-MS to crude oil analysis was soon explored<sup>17</sup> showing great potential as an analytical technique. It was used to investigate mobility trends of crude oil standard constituents, as well as to complement information obtained from FTICR-MS analysis.<sup>31</sup>

Very recently, a new commercial QTOF mass spectrometer was introduced (Agilent Technologies, Inc., Santa Clara, CA) (Fig. 1).<sup>32</sup> It incorporates a uniform-field drift tube that allows high performance ion mobility with superior resolution ( $R_p$  of *c.a.* 80), sensitivity, and accurate collision cross section measurements. The instrument operates under low-field conditions and uses ion funnel technology to increase ion sampling, providing high quality MS and MS/MS data.

In this work, the ability of this new IM-MS system to provide crude oil and petrofuel characterization was for the first time explored. Specifically, we tested the system for its ability to characterize crude oils as well as a real sample of a crude oil contaminated with a pool of demulsifiers from an onshore exploration process and samples of pure gasoline and gasoline with additives from two major types of Brazilian gasoline.

## 2. Material and methods

### 2.1. Samples and reagents

The crude oils sample was provided by UO-SEAL, Sergipe-Alagoas sedimentary basin, Brazil. The crude oil has an average API gravity of 21 and was identified as C01. The petrofuels (regular gasoline and gasoline with additives) were obtained from gas stations in the city of Campinas, São Paulo, Brazil.

The samples of crude oil and petrofuels were prepared by dissolving 2 mg of the sample in toluene/methanol mixture (1 : 1 v/v) obtaining a final solution of 2 mg mL<sup>-1</sup>. For ESI(+), formic acid (0.1%) was added to facilitate protonation of the basic compounds to yield [M + H]<sup>+</sup> ions. For ESI(−), an aqueous solution of 0.1% ammonium hydroxide was added to facilitate deprotonation of the more acidic components to yield [M − H]<sup>−</sup> ions. HPLC-grade methanol, toluene, ammonium hydroxide and formic acid were purchased from Merck S.A. (Rio de Janeiro, Brazil) and used without further purification.

### 2.2. FTICR-MS analysis

The ESI-FTICR-MS analysis was performed using a 7.2T LTQ FT Ultra mass spectrometer (Thermo Scientific, Bremen, Germany) equipped with a direct infusion electrospray ionization source (ESI) operating in the positive and negative ion mode at the following conditions: capillary voltage 3.5 and −3.1 kV, tube lens + and −160 V, temperature 280 °C and for MS/MS fragmentation energy 15–40 eV, respectively. Nitrogen was used as nebulization gas. Mass resolving power was  $m/\Delta m_{50\%} = 400\,000$  at  $m/z$  400 and acquisition in the ICR cell was done with 100  $\mu$ scans (averaged transients) per run. Data acquisition was performed along the  $m/z$  range of 100–2000 by the Xcalibur 2.0 software.

The identification of ions occurred by comparing the  $m/z$  values of peaks obtained from positive and negative ESI-FTICR-MS spectra with a library of compounds in the software PetroMS based on literature search and standards. The PetroMS working process is described elsewhere.<sup>22</sup> We considered a match between the experimental  $m/z$  value and the theoretical  $m/z$  value from our library when the mass error was <1 ppm.

### 2.3. IM-MS analysis

The IM-MS experiments were performed using the new Agilent G6560A (Agilent Technologies Inc., Santa Clara, CA) ion mobility quadrupole time-of-flight (IM-QTOF) system enabling high performance ion mobility, and very precise and accurate collision cross-section (CCS or Ω) measurements without class dependent calibration standards. This IM-QTOF instrument operates under uniform low field conditions, allowing the drift time information for ions to be directly converted to collision cross-section information. The innovative ion funnel technology in this instrument has been demonstrated to dramatically increase the ion sampling into the mass spectrometer resulting in higher quality MS/MS spectra at trace levels.<sup>32</sup> The Agilent ion mobility system consists of a front funnel, trapping funnel, drift tube, and a rear funnel that couples *via* a hexapole to the Q-TOF mass analyzer. The front funnel operates at high pressure where funnel DC and RF voltages help to transfer ions toward the trapping funnel. The key functions of the front ion funnel are to enrich the sample ions and remove excess gas. The continuous ion beam from the electrospray process has to be converted into a pulsed ion beam prior to ion mobility separation. The trapping funnel operates by storing then releasing discrete packets of ions into the drift cell. Ions are separated as they pass through the ion mobility cell based on their size and charge.

The Agilent jet stream ionization source was used for all IM-MS experiments. Operating conditions were as follows: gas temperature: 350 °C, drying gas: 10 L min<sup>-1</sup>, nebulizer pressure: 30 psi, sheath gas temperature: 300 °C, sheath gas flow: 12 L min<sup>-1</sup>, VCap: 3500 V and nozzle voltage: 2000 V. For the IM-MS experiments, acquisition conditions were: drift tube pressure 3.95 Torr, max drift time 60 msec, trap fill time 20 msec, drift tube field strength 18.59 V cm<sup>-1</sup>. Nitrogen was used as the drift gas. Data acquisition was performed using the mass range of 50–2000  $m/z$ . All the mass spectra obtained were accumulated and processed *via* the MassHunter Workstation Software, B.06.00 version.

### 3. Results and discussion

#### 3.1. Crude oils

To test the performance of the new Agilent IM-MS instrument for crude oil analysis, we selected from our inventory of samples, a few samples that represent the most typical, uncontaminated crude oils available with varying geochemical properties<sup>33</sup> as well as, as a test case, a real sample of a crude oil known to be contaminated with unknown demulsifiers. Both CO<sub>2</sub> (ref. 23 and 31) and N<sub>2</sub> were evaluated as drift gases. Since the initial experiments using these two drift gases show no

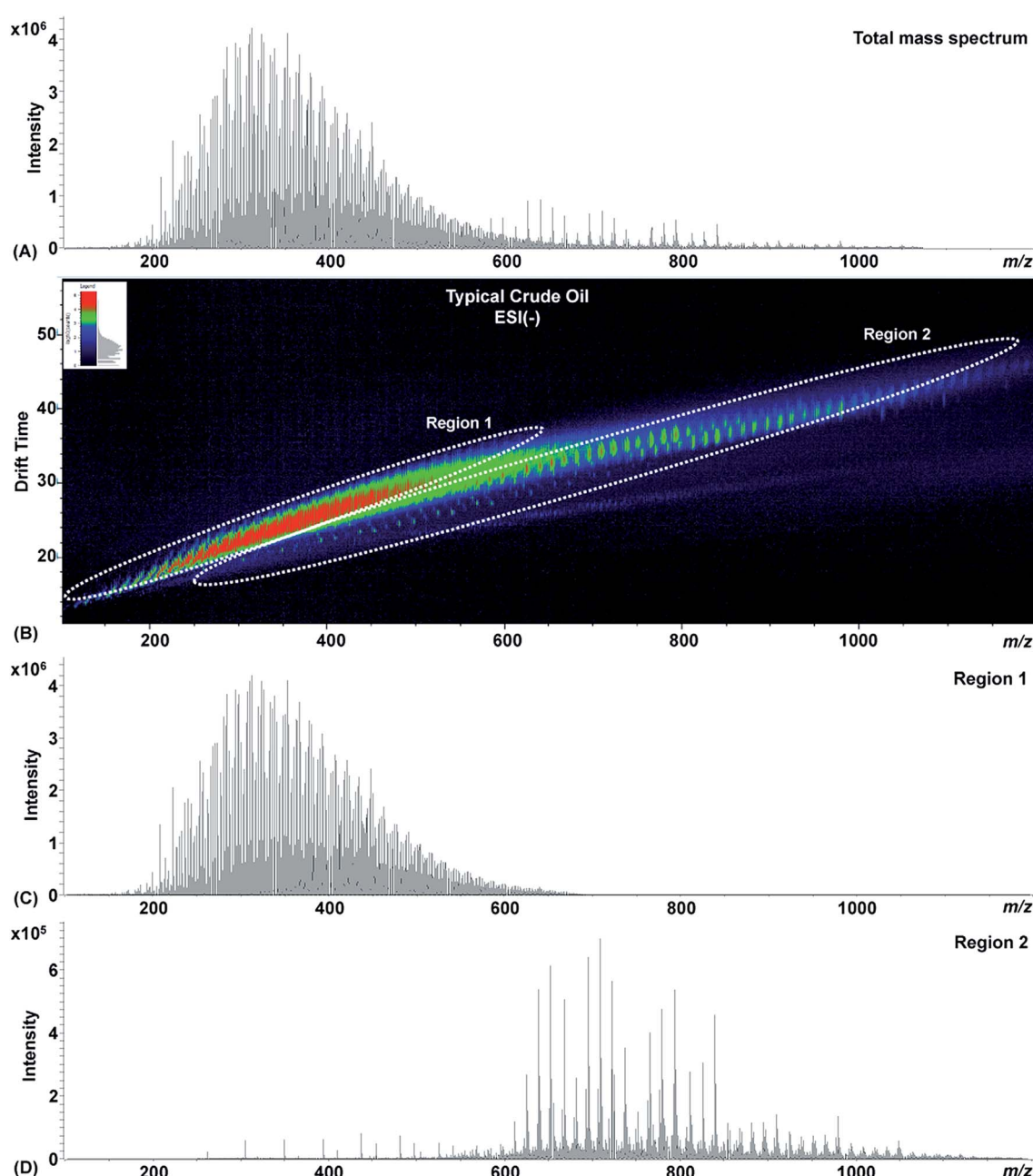


Fig. 2 ESI(–)-IM-MS data for a typical crude oil sample. (A) Total ion mass spectrum, (B) drift time vs.  $m/z$  heat map and (C and D) extracted ion mass spectra for the regions 1 and 2 indicated in (B), respectively.

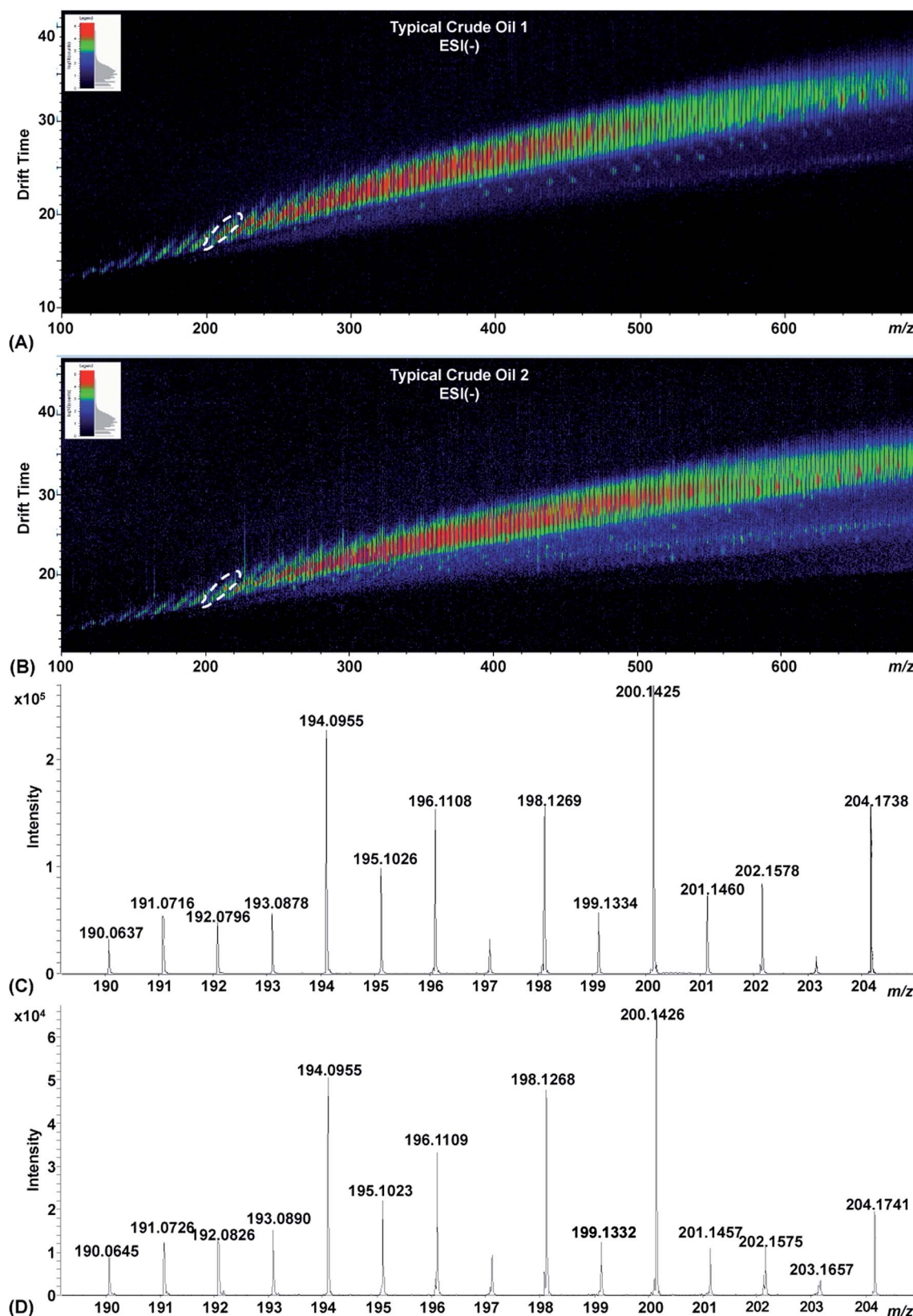


Fig. 3 Drift time versus  $m/z$  heat maps for typical (A) crude oil 1 and (B) crude oil 2 and (C, D) their respective extracted mass spectra.

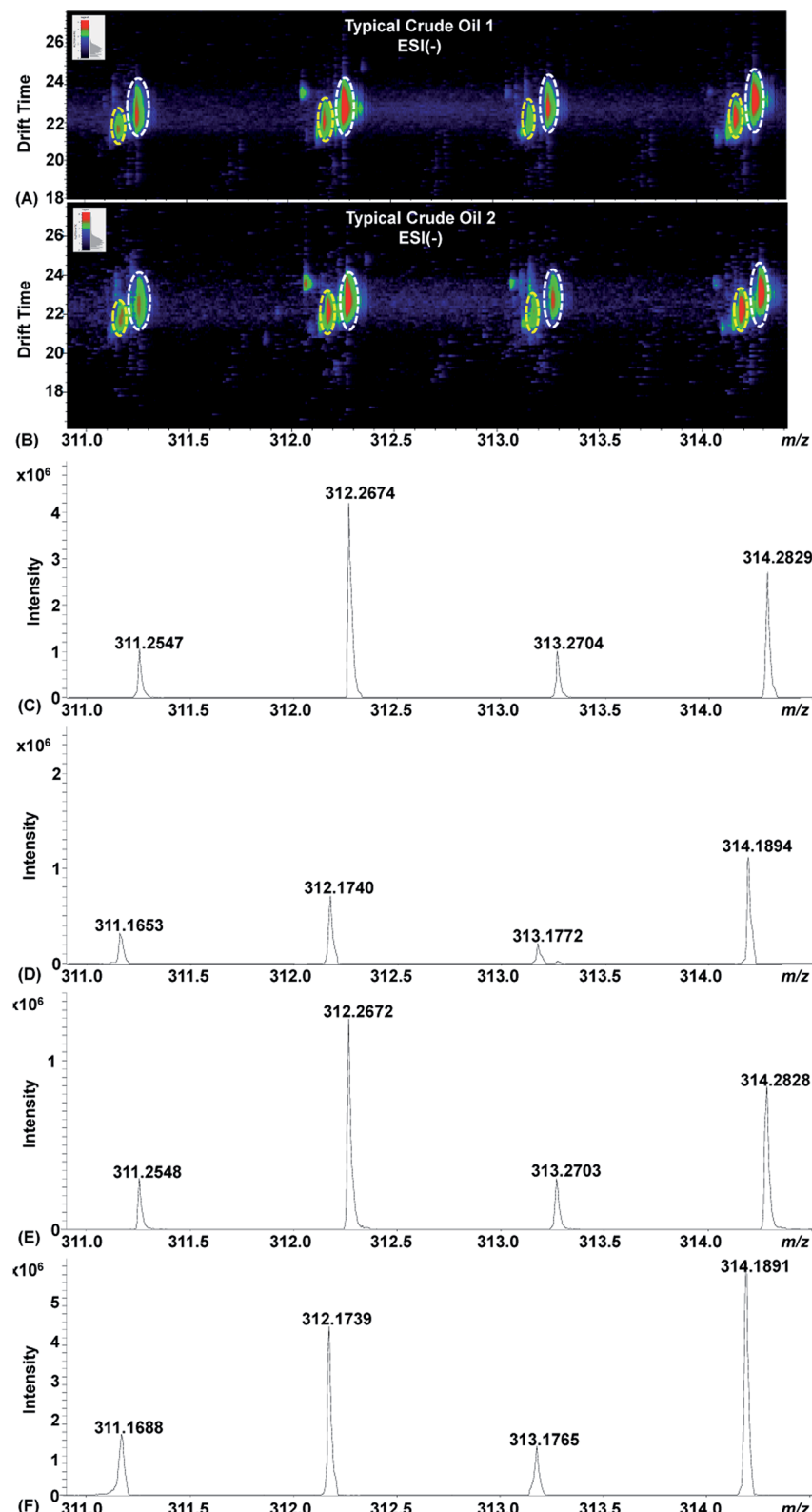


Fig. 4 (A) Drift time versus  $m/z$  heat maps for typical crude oil 1 and (B) typical crude oil 2. (C and D) The extracted ion mass spectra for the white and yellow regions indicated in (A), respectively. (E and F) The extracted ion mass spectra for the white and yellow regions indicated in (B), respectively.

significant differences in ion mobility separation for N<sub>2</sub> or CO<sub>2</sub>, N<sub>2</sub> was selected as the drift gas.

Fig. 2 shows the ESI(–) spectra for a typical crude oil sample, Fig. 2A shows the summed spectrum for both region 1 and region 2 indicated in Fig. 2 (heat map) whereas Fig. 2C shows the ESI(–)spectrum extracted from region 1 indicated in Fig. 2B.

This region shows the well-behaved Gaussian-like distribution of the typical polar markers of crude oils, mostly nitrogen and oxygen containing compounds. Fig. 2D shows the extracted mass spectrum from region 2 indicated in Fig. 2B which corresponds to the contaminants present in this sample. The ion mobility apparatus clearly separated the ions from typical

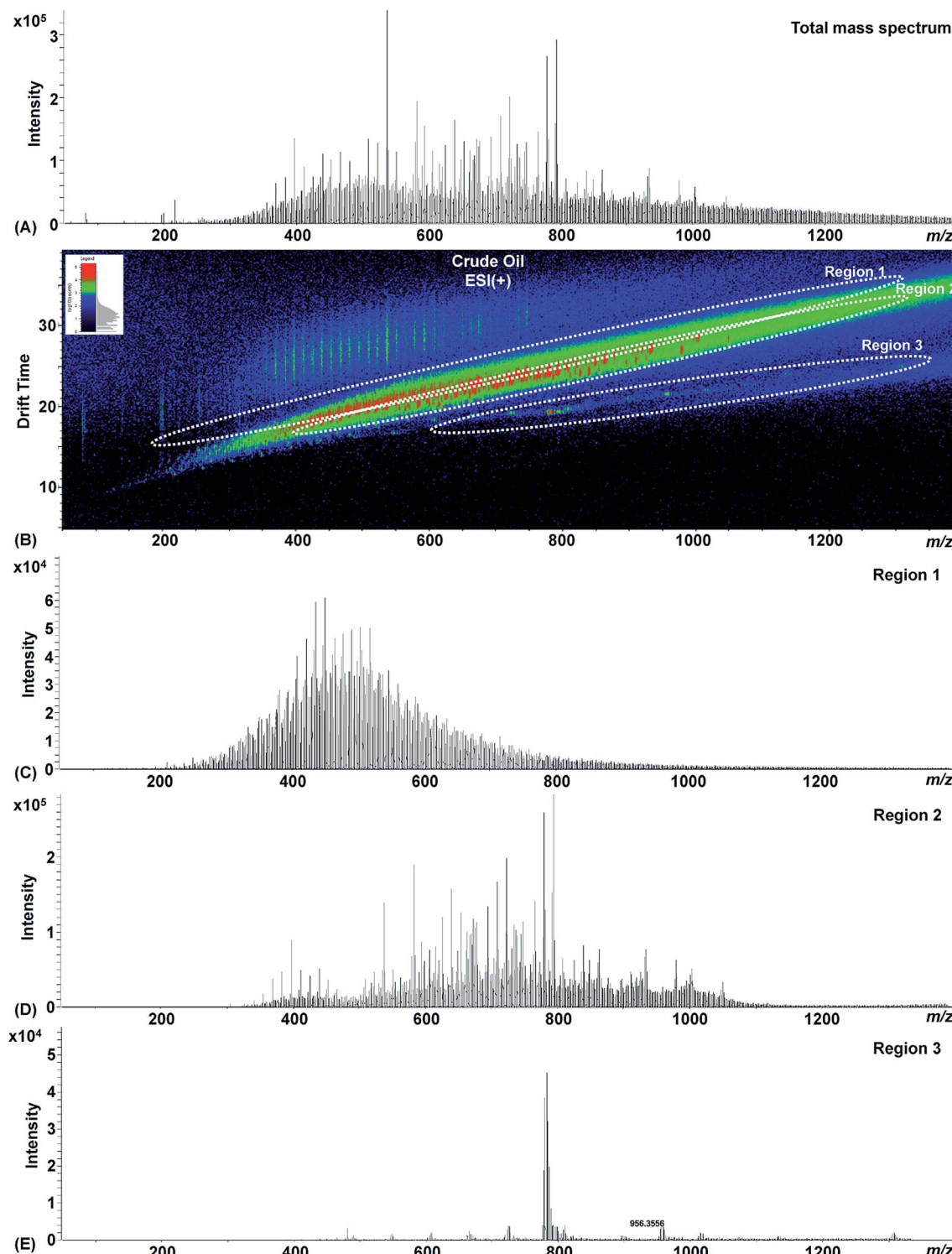


Fig. 5 (A) ESI(+)–IM–MS data for a crude oil sample. Total ion mass spectrum, (B) drift time vs.  $m/z$  heat map and (C–E) extracted ion mass spectra for the regions 1 through 3 indicated in (B), respectively.

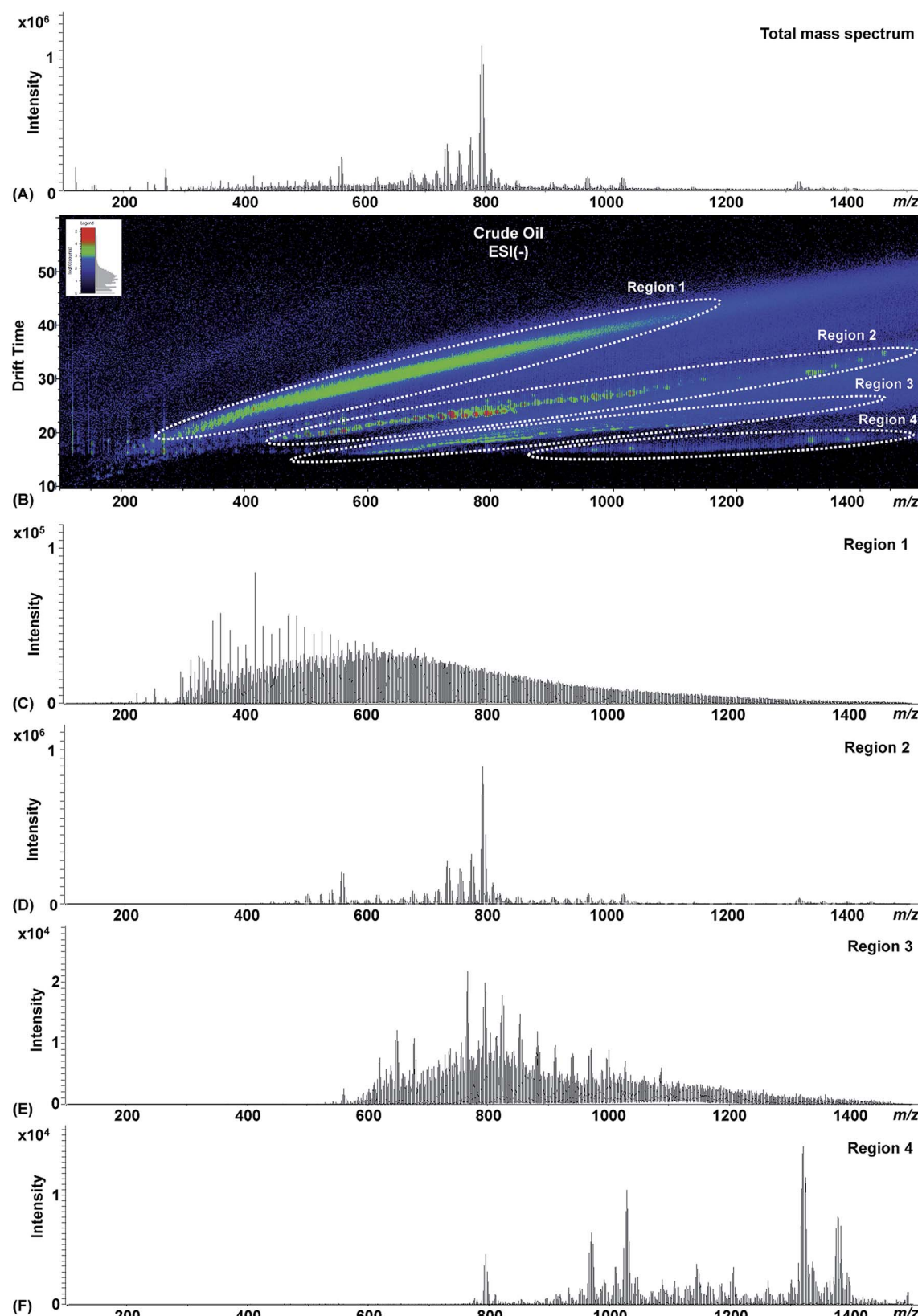


Fig. 6 ESI<sup>(−)</sup>-IM-MS data for a crude oil sample. (A) Total ion mass spectrum, (B) drift time vs.  $m/z$  heat map and (C–F) extracted ion mass spectra for the regions 1 through 4 indicated in (B), respectively.

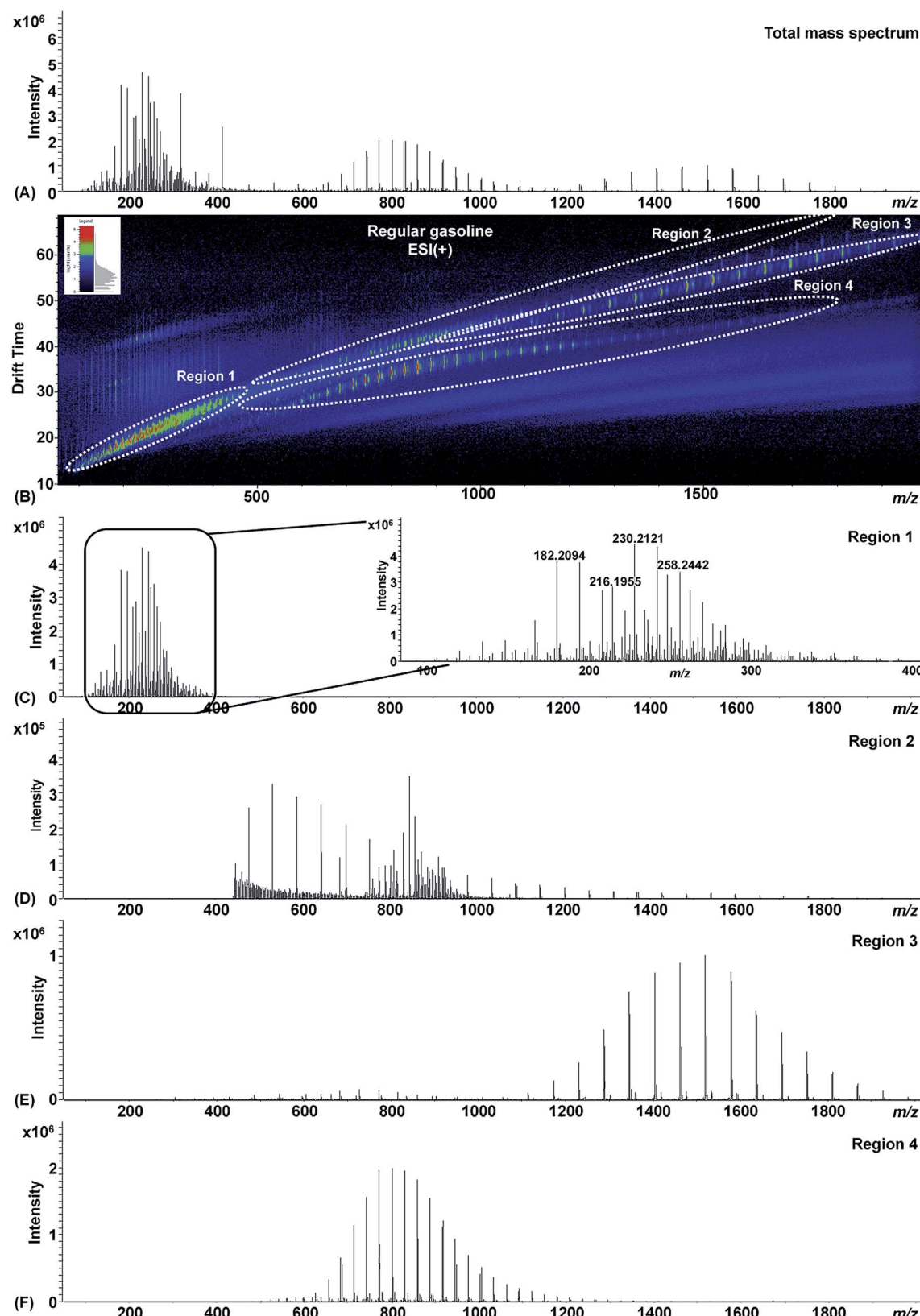


Fig. 7 ESI(+)–IM–MS data for regular gasoline. (A) Total ion mass spectrum, (B) drift time vs.  $m/z$  heat map and (C–F) extracted ion mass spectra for the regions 1 through 4 indicated in (B), respectively.

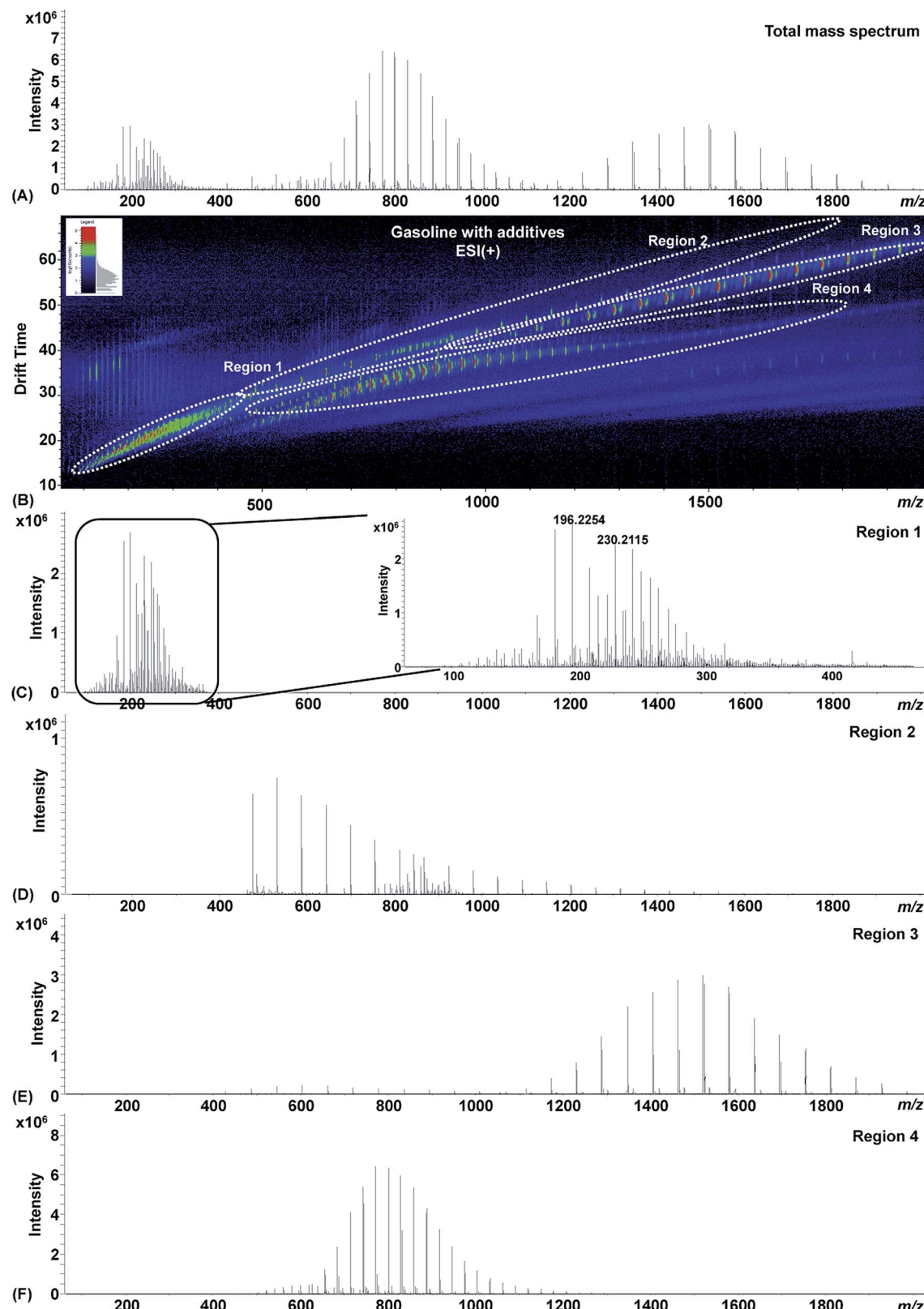


Fig. 8 ESI(+)–IM–MS data for gasoline with additives. (A) Total ion mass spectrum, (B) drift time vs.  $m/z$  heat map and (C–F) extracted ion mass spectra for the regions 1 through 4 indicated in (B), respectively.

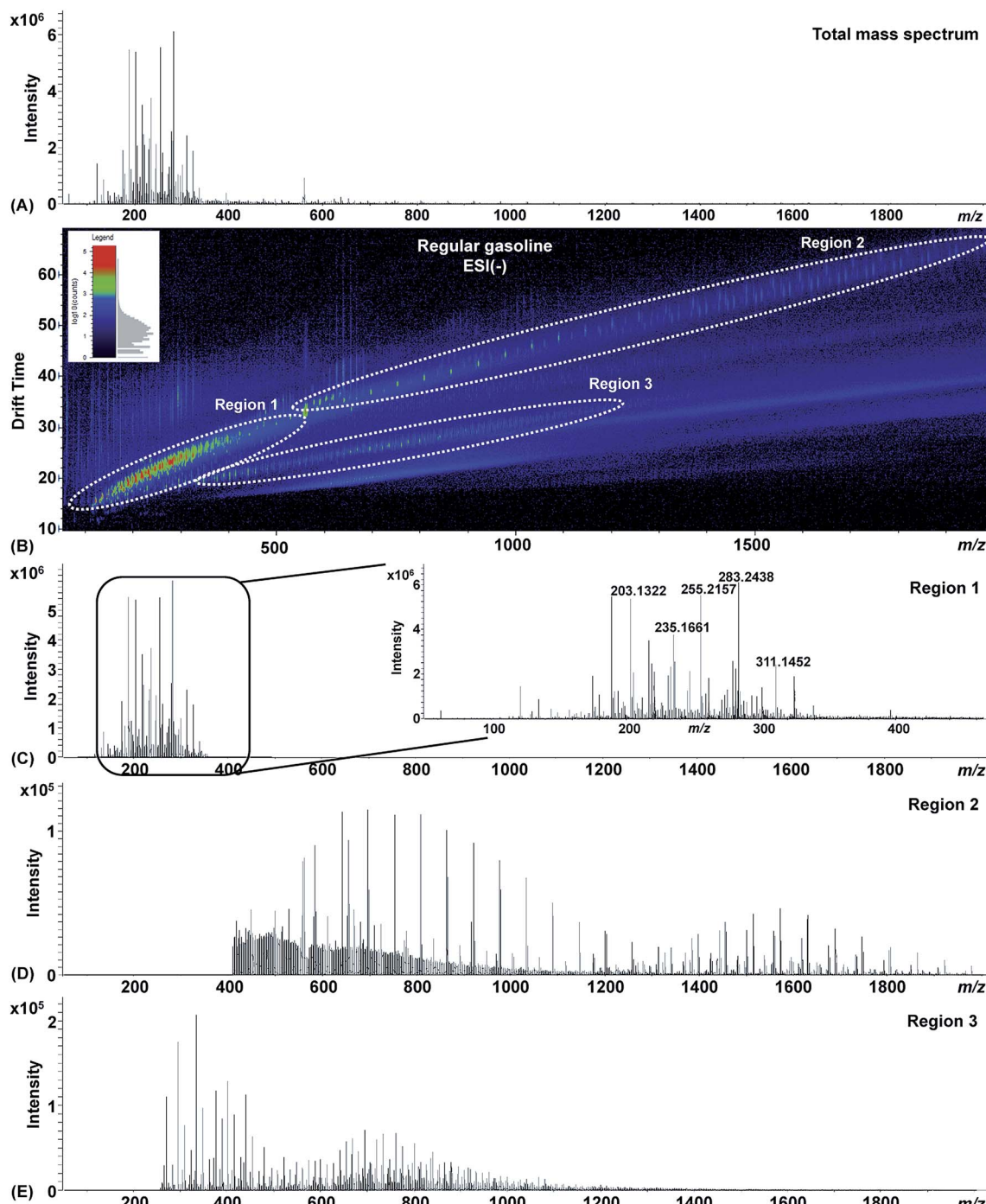


Fig. 9 ESI( $-$ )-IM-MS data for a sample of regular gasoline. (A) Total ion mass spectrum, (B) drift time vs.  $m/z$  heat map and (C–E) extracted ion mass spectra for the regions 1 through 3 indicated in (B), respectively.

constituents of crude oils from those of the contaminants which belong to a different class. Note that the contaminant ions fall on a different trend line as compared to the crude oil constituents (region 1 vs. region 2 in Fig. 2B).

In the heat map “band” of two crude oil samples of Fig. 3A and B, the well-resolved  $C_n$  homologue series is represented by parallel “ladders” separated from each other by 14 Da units, whereas the “stair-like” DBE profiles within each ladder are separated by 2 Da each. Note also that DBE comparison

(unsaturation level) of both crude oil samples can be performed by extracting the respective spectrum for each  $C_n$  ladder, as indicated by the spectra of Fig. 3C and D. For sample 2 (Fig. 3D), a higher unsaturation level than that of sample 1 (Fig. 3C) is indicated by the greater relative abundances of higher DBE ions.

“Base line” resolution can however only be obtained for the  $C_n$  ladders below  $m/z$  250, and above that  $m/z$ ,  $C_n$  ladders seem to overlap as the  $m/z$  increases. This apparent overlap is

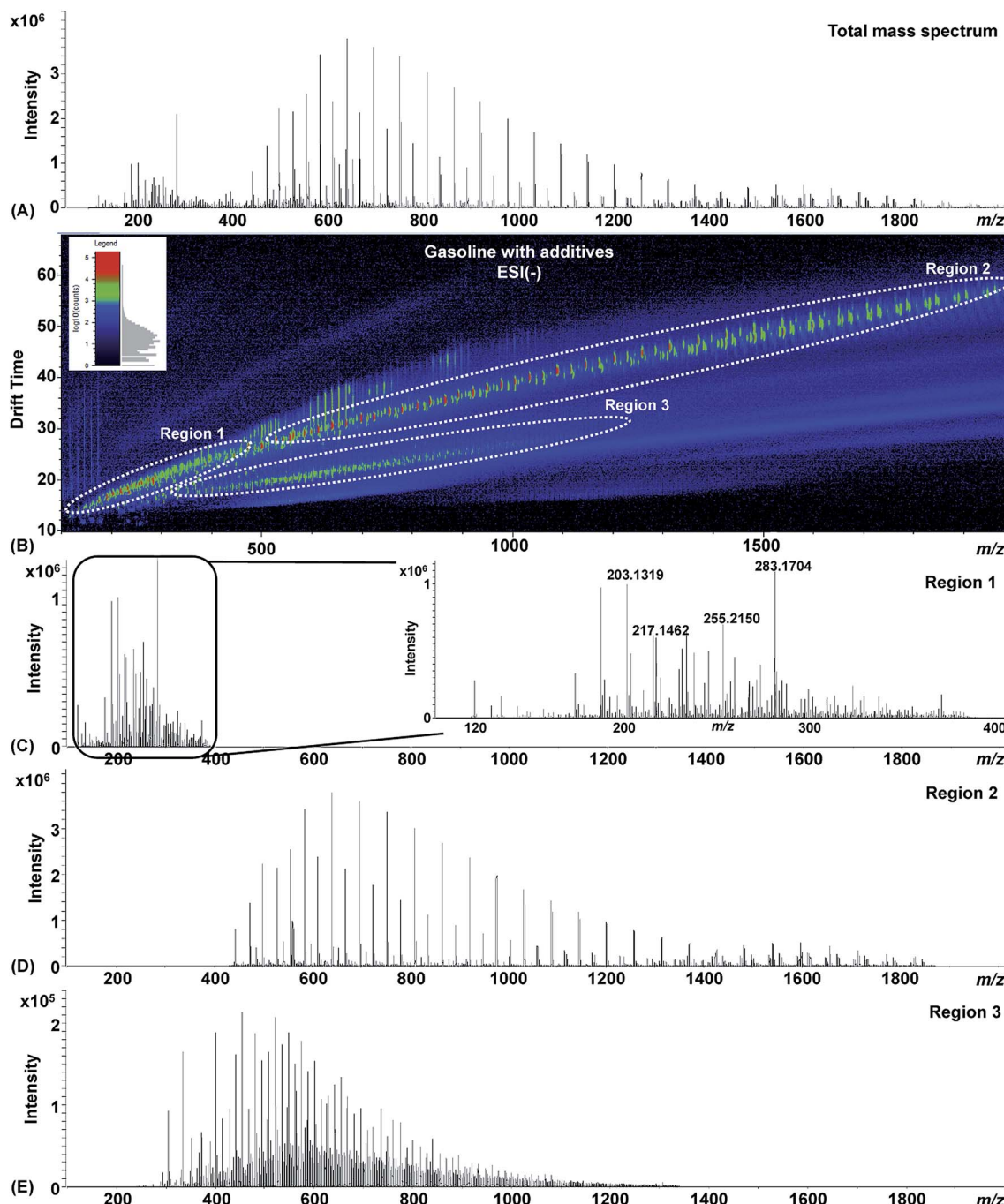


Fig. 10 ESI( $-$ )-IM-MS data for gasoline with additives. (A) Total ion mass spectrum, (B) drift time vs.  $m/z$  heat map and (C–E) extracted ion mass spectra for the regions 1 through 3 indicated in (B), respectively.

demonstrated by the visual merging of the 2D space in the heat map that corresponds to  $C_n$  (DBE = 4, longer drift time) with that of the 2D space in the heat map that corresponds to the  $C_{n+1}$  (DBE = 10, shorter drift time). As Fig. 4 shows, the drift profiles display properly separate ions from both ladders throughout the whole heat map band.

Fig. 5 and 6 show the ESI(+)-IM-MS and ESI( $-$ )-IM-MS data of a real crude oil sample contaminated with demulsifiers. ESI(+)-MS and ESI( $-$ )-MS without IM separation produce quite poor spectra (Fig. 5A and 6B), which display insufficient MS

resolution to separate overlaid peaks and the Gaussian profile for crude oil ions is present but obscured by ions from contaminants, in particular, the demulsifier ions. When IM separation is used in conjunction with MS and proper regions are selected, much cleaner and typical crude oil spectra are however produced (Fig. 5C and 6C), which are nearly free of contaminant ions. The strategies previously described for comparing  $C_n$  ladders in terms of DBE trends (Fig. 3 and 4) of the non-contaminated crude oil sample can therefore also be applied to heavily contaminated samples. In addition, a

number of spectra (Fig. 5D, E and Fig. 6D–F) for series of contaminants obtained *via* both ESI(+) and ESI(−) can be properly resolved from selected mobility regions, and can be used for more appropriate characterization of the demulsifiers.

Regions 2 and 3 in Fig. 6D and E, for instance, produced spectra in which a homologous series of contaminants with ions 28 *m/z* units apart are attributed to C<sub>2</sub>H<sub>4</sub> units of fatty acid chains. Note that indeed copolymers of fatty acids are frequently used as surfactants by the petrochemical industries.<sup>34</sup> Region 4 shows a spectrum (Fig. 6F) in which ions are separated by 58 *m/z* units which can be related to propylene oxide (PO) units of PO based surfactants. Their average MW and mass dispersion can be easily inferred from these clean, high quality spectra.

A toluene–methanol solution of the typical crude oil sample contaminated with demulsifiers was made and analyzed using a high resolution FTICR-MS instrument. This instrument consists of a 7.2 T magnet and was operated at a *R*<sub>p</sub> of 400 000@*m/z* 400. A high abundance of contaminant ion peaks

seriously hampered the data analysis, preventing the proper ion classification in both ESI(+) and ESI(−) modes (Fig. S1†).

### 3.2. Petrofuels

Samples from the two most typical types of Brazilian gasoline:<sup>35</sup> regular (RG) and gasoline with additives (AG), were also analyzed by ESI(±)-IM-MS to investigate the ability of the new IM drift cell to provide the proper separation of additives (Fig. 7–10).

For both RG and AG samples, classes of constituents appearing together in the ESI(±) spectra (Fig. 7A, 8A, 9A and 10A) were indeed efficiently separated by IM. Region 1 for both samples display spectra with the typical distribution of the homologous series of alkyl pyridines detected in gasoline by ESI(+)<sup>31</sup> and alkyl pyrroles by ESI(−).<sup>36</sup> IM was also able to resolve several classes of additives, with their extracted spectra from specific regions allowing proper characterization of these gasoline additives or contaminants in both ESI(+) and ESI(−) modes. For example, the +58 Da (Fig. 7E, region 3) and +28 Da

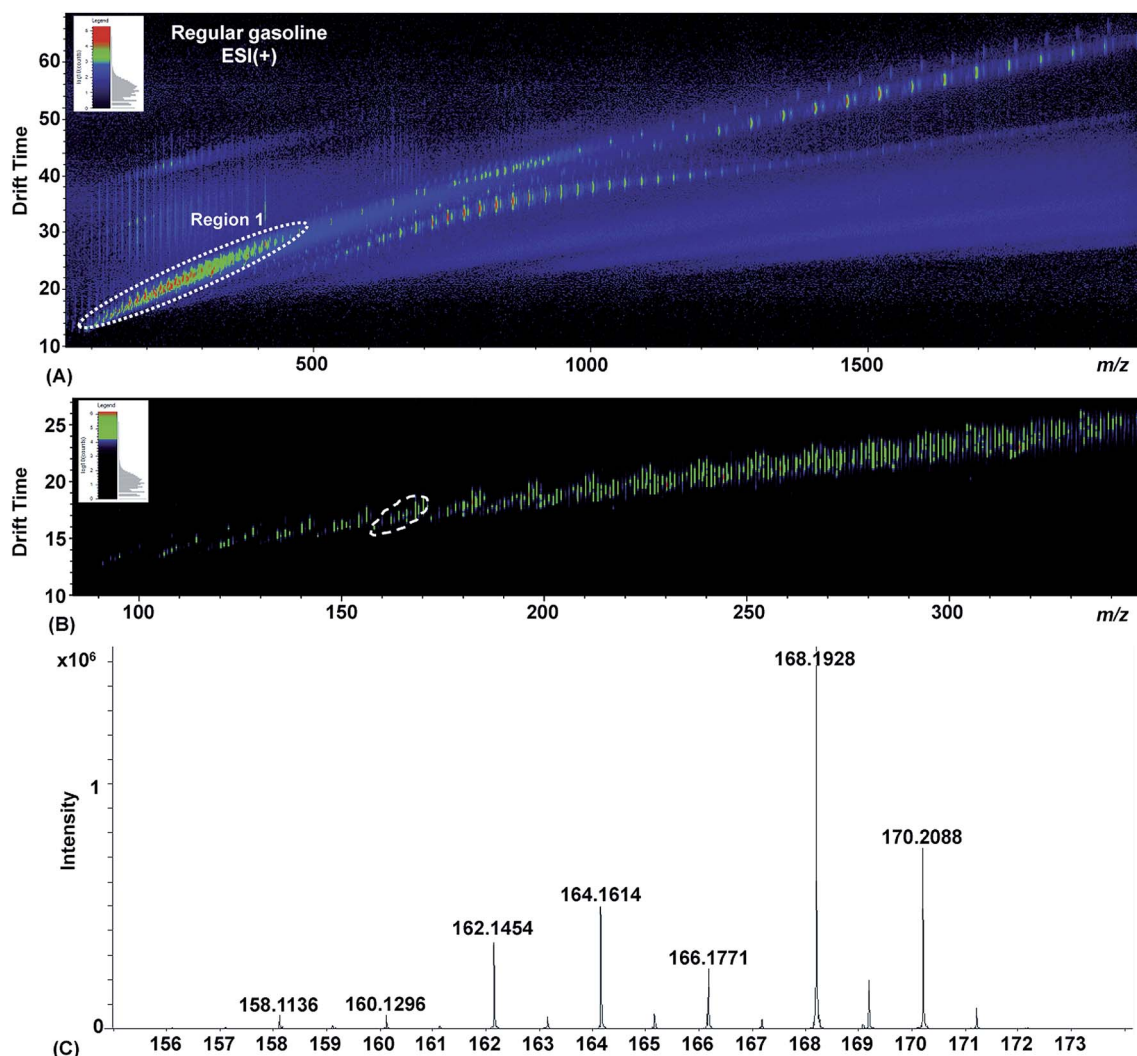


Fig. 11 (A) ESI(+) IM-MS drift time versus *m/z* heat map for regular gasoline, (B) extended ATD enlargement of region 1 and (C) their respective extracted spectrum.

(Fig. 7F, region 4) oligomeric series attributed to PO and fatty acid based surfactants respectively, with very well defined MW profiles.

As Fig. 11 shows, the typical polar composition of the gasoline itself could also be characterized by investigating the two-dimensional features observed in the heat map and the extracted mass spectra for the DBE trends in each  $C_n$  ladder.

## 4. Conclusions

IM-MS experiments performed using the new Agilent IM-QTOF instrument showed detailed composition features of crude oils, gasoline and their contaminants and additives that were not discernible *via* MS only experiments. The high IM resolution provided by this instrument enables the separation of selected ESI spectra and therefore the proper MS characterization of crude oil and petrofuels apart from their contaminants and additives. These results further demonstrate the power of IM-MS as a complementary technique in MS petroleomics with several potential applications for the petrochemical industry. Note that it seems possible, by using standards for additives and contaminants, to perform not only the separation and characterization but also a semi-quantitative evaluation of their relative concentrations. In gasoline, the much higher ESI(+) and/or ESI(−) detectability of additive ions, as compared to those of the gasoline marker ions, makes their detection and semi-quantitation, after IM separation, perfectly feasibly.

## Acknowledgements

We would like to thank the Fundação de Amparo a Pesquisa do Estado de São Paulo (FAPESP) for the scholarship awarded to J.M.S. (process number 2013/19161-4), Coordenação de Aperfeiçoamento de Pessoal de Nível Superior (CAPES) and Conselho Nacional de Desenvolvimento Científico e Tecnológico (CNPq) (Brazilian research councils) for fellowships. We also acknowledge Petrobras (Petróleo Brasileiro) for financial support.

## References

- B. M. F. Ávila, B. G. Vaz, R. Pereira, A. O. Gomes, R. C. L. Pereira, Y. E. Corilo, R. C. Simas, H. D. L. Nascimento, M. N. Eberlin and D. A. Azevedo, Comprehensive chemical composition of gas oil cuts using two-dimensional gas chromatography with time-of-flight mass spectrometry and electrospray ionization coupled to fourier transform ion cyclotron resonance mass spectrometry, *Energy Fuels*, 2012, **26**, 5069–5079.
- K. A. P. Colati, G. P. Dalmaschio, E. V. R. Castro, A. O. Gomes, B. G. Vaz and W. Romão, Monitoring the liquid/liquid extraction of naphthenic acids in brazilian crude oil using electrospray ionization FTICR mass spectrometry (ESI FTICR MS), *Fuel*, 2013, **108**, 647–655.
- R. Martínez-Palou, R. Cerón-Camacho, B. Chávez, A. A. Vallejo, D. Villanueva-Negrete, J. Castellanos, J. Karamath, J. Reyes and J. Aburto, Demulsification of heavy crude oil-in-water emulsions: A comparative study between microwave and thermal heating, *Fuel*, 2013, **113**, 407–414.
- M. Meriem-Benziane, S. A. Abdul-Wahab, M. Benaicha and M. Belhadri, Investigating the rheological properties of light crude oil and the characteristics of its emulsions in order to improve pipeline flow, *Fuel*, 2012, **95**, 97–107.
- R. P. Rodgers, T. M. Schaub and A. G. Marshall, Petroleomics: MS returns to its roots, *Anal. Chem.*, 2005, **77**, 20A–27A.
- S. Chiaberge, T. Fiorani, A. Savoini, A. Bionda, S. Ramello, M. Pastori and P. Cesti, Classification of crude oil samples through statistical analysis of APPI FTICR mass spectra, *Fuel Process. Technol.*, 2013, **106**, 181–185.
- B. G. Vaz, R. C. Silva, C. F. Klitzke, R. C. Simas, H. D. L. Nascimento, R. C. L. Pereira, D. F. Garcia, M. N. Eberlin and D. A. Azevedo, Assessing biodegradation in the llanos orientales crude oils by electrospray ionization ultrahigh resolution and accuracy fourier transform mass spectrometry and chemometric analysis, *Energy Fuels*, 2013, **27**, 1277–1284.
- S. Poetz, B. Horsfield and H. Wilkes, Maturity-driven generation and transformation of acidic compounds in the organic-rich posidonia shale as revealed by electrospray ionization fourier transform ion cyclotron resonance mass spectrometry, *Energy Fuels*, 2014, **28**, 4877–4888.
- B. G. Vaz, P. V. Abdelnur, W. F. C. Rocha, A. O. Gomes and R. C. L. Pereira, Predictive petroleomics: measurement of the total acid number by electrospray fourier transform mass spectrometry and chemometric analysis, *Energy Fuels*, 2013, **27**, 1873–1880.
- S. Kelesoglu, B. H. Pettersen and J. Sjöblom, Flow properties of water-in-north sea heavy crude oil emulsions, *J. Pet. Sci. Eng.*, 2012, **100**, 14–23.
- N. H. Roodbari, A. Badiei, E. Soleimani and Y. Khaniani, Tweens demulsification effects on heavy crude oil/water emulsion, *Arabian J. Chem.*, 2011, *in press*.
- G. Mohebali, A. Kaytash and N. Etemadi, Efficient breaking of water/oil emulsions by a newly isolated de-emulsifying bacterium, *Ochrobactrum anthropi* strain RIPI5-1, *Colloids Surf. B*, 2012, **98**, 120–128.
- N. N. Zaki, M. E. Abdel-Raouf and A. A. Abdel-Azim, Propylene oxide–ethylene oxide block copolymers as demulsifiers for water-in-oil emulsions, I. effect of molecular weight and hydrophilic–lipophilic balance on the demulsification efficiency, *Monatsh. Chem.*, 1996, **127**, 621–629.
- W. Kang, G. Jing, H. Zhang, M. Li and Z. Wu, Influence of demulsifier on interfacial film between oil and water, *Colloids Surf. A*, 2006, **272**, 27–31.
- D. Daniel-David, I. Pezon, C. Dalmazzone, C. Noik, D. Clausse and L. Komunjer, Elastic properties of crude oil/water interface in presence of polymeric emulsion breakers, *Colloids Surf. A*, 2005, **270–271**, 257–262.
- R. A. Mohammed, A. I. Bailey, P. F. Luckham and S. E. Taylor, Dewatering of crude oil emulsions, *Colloids Surf. A*, 1994, **83**, 261–271.

- 17 F. A. Fernandez-Lima, C. Becker, A. M. McKenna, R. P. Rodgers, A. G. Marshall and D. Russell, Petroleum crude oil characterization by TWIM-MS and FTICR MS, *Anal. Chem.*, 2009, **81**, 9941–9947.
- 18 J. G. Speight, *The Chemistry and technology of petroleum*, CRC Press, Boca Raton, FL, 4th edn, 2006.
- 19 Q. Shi, D. Hou, K. H. Chung, C. Xu, S. Zhao and Y. Zhang, Characterization of heteroatom compounds in a crude oil and its saturates, aromatics, resins, and asphaltenes (SARA) and non-basic nitrogen fractions analyzed by negative-ion electrospray ionization fourier transform ion cyclotron resonance mass spectrometry, *Energy Fuels*, 2010, **24**, 2545–2553.
- 20 C. F. Klitzke, Y. E. Corilo, K. Siek, J. Binkley, J. Patrick and M. N. Eberlin, Petroleomics by ultrahigh-resolution time-of-flight mass spectrometry, *Energy Fuels*, 2012, **26**, 5787–5794.
- 21 K. O. Zhurov, A. N. Kozhinov and Y. O. Tsybin, Evaluation of high-field orbitrap fourier transform mass spectrometer for petroleomics, *Energy Fuels*, 2013, **27**, 2974–2983.
- 22 Y. E. Corilo, B. G. Vaz, R. C. Simas, H. D. L. Nascimento, C. F. Klitzke, R. C. L. Pereira, W. L. Bastos, E. V. Santos Neto, R. P. Rodgers and M. N. Eberlin, Petroleomics by EASI( $\pm$ ) FTICR MS, *Anal. Chem.*, 2010, **82**, 3990–3996.
- 23 M. Fasciotti, P. M. Lalli, G. Heerdt, R. A. Stefen, Y. E. Corilo, G. F. de Sá, R. J. Daroda, F. A. M. Reis, N. H. Morgan, R. C. L. Pereira, M. N. Eberlin and C. F. Klitzke, Structure-drift time relationships in ion mobility mass spectrometry, *Int. J. Ion Mobility Spectrom.*, 2013, **16**, 117–132.
- 24 J. Ponthus and E. Riches, Evaluating the multiple benefits offered by ion mobility-mass spectrometry in oil and petroleum analysis, *Int. J. Ion Mobility Spectrom.*, 2013, **16**, 95–103.
- 25 E. W. McDaniel, D. W. Martin and W. S. Barners, Drift tube-mass spectrometer for studies of low-energy ion-molecule reactions, *Rev. Sci. Instrum.*, 1962, **33**(2), 2–7.
- 26 P. R. Kemper and M. T. Bowers, A hybrid double-focusing mass spectrometer-high-pressure drift reaction cell to study thermal energy reactions of mass-selected ions, *J. Am. Soc. Mass Spectrom.*, 1990, **1**, 197–207.
- 27 H. H. Hill, W. F. Siems and R. H. S. Louis, Ion mobility spectrometry, *Anal. Chem.*, 1990, **23**, 1201A–1209A.
- 28 F. W. Karasek, M. J. Cohen and D. I. Carroll, Trace studies of alcohols in the plasma chromatography-mass spectrometer, *J. Chromatogr. Sci.*, 1971, **9**, 390–392.
- 29 K. Giles, S. D. Pringle, K. R. Worthington, D. Little, J. L. Wildgoose and R. H. Bateman, Applications of a travelling wave-based radio-frequency-only stacked ring ion guide, *Rapid Commun. Mass Spectrom.*, 2004, **18**, 2401–2414.
- 30 S. D. Pringle, K. Giles, J. L. Wildgoose, J. P. Williams, S. E. Slade, K. Thalassinos, R. H. Bateman, M. T. Bowers and J. H. Scrivens, An investigation of the mobility separation of some peptide and protein ions using a new hybrid quadrupole/travelling wave IMS/oa-TOF instrument, *Int. J. Ion Mobility Spectrom.*, 2007, **261**, 1–12.
- 31 M. Fasciotti, P. M. Lalli, C. F. Klitzke, Y. E. Corilo, M. A. Pudenzi, R. C. L. Pereira, W. Bastos, R. J. Daroda and M. N. Eberlin, Petroleomics by traveling wave ion mobility–mass spectrometry using CO<sub>2</sub> as a drift gas, *Energy Fuels*, 2013, **27**, 7277–7286.
- 32 R. Kurulugama, K. Imatani and L. Taylor, *Technical overview: The Agilent ion mobility Q-TOF mass spectrometer system*, Agilent Technologies, 2013.
- 33 R. C. L. Pereira, R. C. Simas, Y. E. Corilo, B. G. Vaz, C. F. Klitzke, E. M. Schimdt, M. A. Pudenzi, R. M. C. F. Silva, E. T. Moraes, W. L. Bastos, M. N. Eberlin and H. D. L. Nascimento, Precision in petroleomics via ultrahigh resolution electrospray ionization fourier transform ion cyclotron resonance mass spectrometry, *Energy Fuels*, 2013, **27**, 7208–7216.
- 34 Z. H. Asadov, A. H. Tantawy, A. H. Azizov, I. A. Zarbaliyeva and R. A. Rahimov, Synthesis of new complexes surfactants based on fatty acids and study the effect of lenght of fatty acid chain on the petroleum and surface-active properties, *Caspian Journal of Applied Sciences Research*, 2013, **2**(3), 24–34.
- 35 National Agency of Petroleum, Natural Gas and Biofuels of Brazil, ANP resolution no.40, de 25.10.2013, Brazil, <http://www.anp.gov.br>, 2013, accessed 20.08.14.
- 36 R. Haddad, T. Regiani, C. F. Klitzke, G. B. Sanvido, Y. E. Corilo, D. V. Augusti, V. M. D. Pasa, R. C. C. Pereira, W. Romão, B. G. Vaz, R. Augusti and M. N. Eberlin, Gasoline, kerosene, and diesel fingerprinting via polar markers, *Energy Fuels*, 2012, **26**(6), 3542–3547.